UNIVERSITY OF WEST BOHEMIA

Applied and Computational Mechanics 1 (2007) 437 - 444

Applied and Computational Mechanics

Aerosol deposition in human airways during breathing cycle

M. Forman[a], M. Jícha[a,*], J. Katolický[a]

[a] *Faculty Mechanical Engineering, BUT, Technická 2, 616 69 Brno, Czech Republic*

Received 10 September 2007; received in revised form 9 October 2007

Abstract

A numerical model of the aerosol transport and deposition in human airways is presented. The model was acquired from a CT scan a living person and consist of 6-9 bifurcations giving around 100 terminations of the tree. The oral/nasal cavity was not modelled in the presented work. The deposition of the particles is given for two breathing regimes, the resting conditions with a tidal volume of 0.5 liter and $15^{l}/_{min}$ ventilation with period of $4^{sec}/_{cycle}$ and full exercise conditions with 3.33 liter tidal volume and $120^{l}/_{min}$ minute ventilation with cycle period of $1.25^{sec}/_{cycle}$. The aerosol concentration was assumed $50^{\mu g}/_{m^3}$ distributed in the three size classes PM10, PM 5 and PM 1. The results shows deposition in different segments of the tracheo-bronchial tree as well as velocity profiles at different time steps of the breathing cycle.

Keywords: aerosol transport, deposition, human airways, CFD

1. Introduction

Computational Fluid Dynamics simulation of airflow and particle transport and deposition in the human respiratory tract has been pursued by a number of researchers. Some recent examples (not exhaustive) are presented in [1] and [3] or [6]. While CFD simulation of the nasopharynx/oropharynx have been quite successful [5], the complexity of the human tracheobronchial tree has defied detailed simulation of airflow in anything else than small sections, e.g. [8] or [2]. Although most of the simulation found in literature presents results for steady-state situation of inhale phase, some transient results with deposition appeared recently [9]. to study the progress of the deposition in subsequent generations of the airways in time, transient simulations has been carried for two breathing regimes, namely resting conditions and maximum exercise.

2. Model description

2.1. Geometry description

The air flow and aerosol deposition has been modelled on a real geometry of a living person using high resolution CT scan from St. Anna hospital in Brno (see fig. 1). The data from the scan has been transformed into triangulated surface mesh using STL format. The mesh was smoothed and cleaned off unnecessary details and by means of an automatic mesh generator first the surface and then the volume meshes were created. The model contains 3.5 million of tetrahedral control volumes with high local refinement in the locations of high velocity gradients. These are namely the location around the bifurcations. At the outlet, pressure conditions (with

*Corresponding author. Tel.: +420 54114 3271, e-mail: jicha@fme.vutbr.cz.

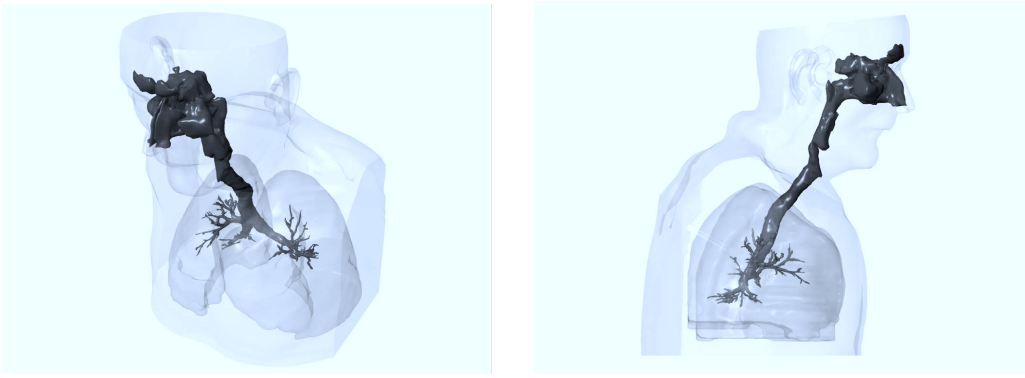

(a) CT scan – frontal view. (b) CT scan – side view.

Fig. 1. CT scan.

given static pressure) were ascribed. For the modeling purposes, the nasal/oral cavity was omitted and the inlet to the airways was placed above the glottis. The solution domain with selected planes in which results were analyzed is shown in fig. 2 (human front view).

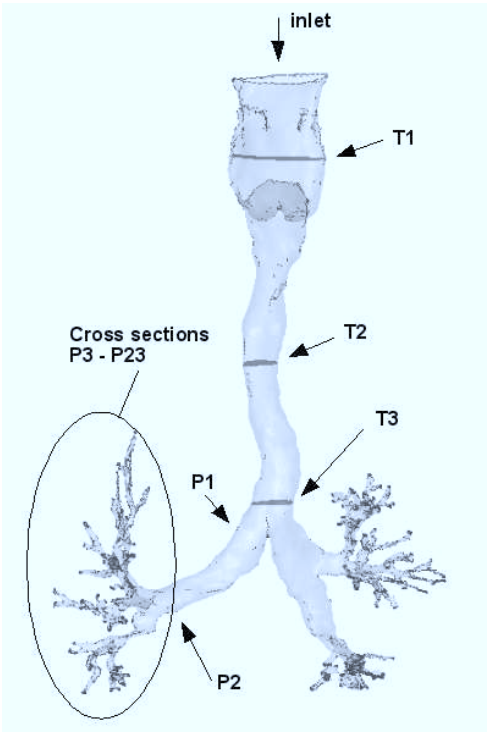

Fig. 2. Computational domain.

Commercial CFD code Star-CD was used for computations using PISO algorithm with second order discretisation in time (Crank–Nichoslon) and space (QUICK) schemes. Calculations were done using low reynolds formulation of $k - \omega$ turbulence model [7] with a hybrid wall function of STAR-CD applied on the rigid walls. The Euler-Lagrange Eddy Interaction Model by Gosman and Ioannides [4] for particles transport has been employed for aerosol particles transport. The particles are injected in three planes, where 60 points for each particle size was defined uniformly supposing strong dispersion effect from the oral/nasal cavity flow.

Two regimes, namely resting conditions and maximum exercise were simulated with the inlet conditions given in tab. 1. Both regimes were calculated in the transient mode consisting of inspiration and expiration that followed a sinusoidal curve according to the formula:

$$V(t) = V_t sin(2\pi f t), \tag{1}$$

where V_t is a tidal volume, f is frequency and t is time. The total volume of the lungs from the CT scan was 4.1 litres. For the aerosol description three size classes were defined, were

	Resting conditions	Maximum exercise
Tidal volume $V_t[liter]$	0.5	3.33
Flow rate $[^{l}/_{min}]$	15	120
Breathing frequency $[Hz]$	0.25	0.8
Period $[s]$	4	1.25

Tab. 1. Modelling scenario.

the concentrations of the different sizes follows the measurements at the street canyon in the city of Brno as shown in tab. 2. The concentration for each class at the inlet is defined to obey the concentrations with respect to the inlet velocity.

Particle diameter $[\mu m]$	Concentration $[^{\mu g}/_{m^3}]$
10	25
5	9
1	16

Tab. 2. Aerosol characteristics.

3. Results

First the flow–field at the maximum inhale velocity (at ¼ of the breathing period) are examined. These results show a slight asymmetry in the flow rate distribution between the left and right airways under both, the resting conditions and maximum exercise. The asymmetry can be seen in fig. 3 where the mass fluxes for resting condition are relative to the mass–flux to the airways as well as the mass–fluxes at the maximum exercise are relative to the mass–flux under the maximum exercise condition. This graph shows that the asymmetry is not influenced by the velocity in the airways except for the right hand side generations 4 and 5 respectively. At both regimes, the flow into the first generation is influenced by the flow pattern just behind the bend upstream, in the plane marked T3 (see fig. 2) that partially blocks the flow into the right airways. Thus we can see for 18 per cent lower flow rate into the right airways. The mass flow gradually decreases as the airways continue to bifurcate and distribute the air flow into the smaller airways. In the fig. 4 and fig. 3. the Reynolds number is shown that reflects not only the flow rate of the air but also the influence of the diameter of the individual airways in the appropriate generation. We can see an increase of the Reynolds number from the first to the second generation which is due to the increase of the velocity in the appropriate generation with the smaller cross section. This increase in the Re number can influence the deposition of aerosols due to changes in the turbulence and thus the aerosol transport characteristics. In the lower generations, the Re number gradually decreases due to both, the airflow

rate and airways diameter reduction. For the maximum exercise, the regime gradually changes from turbulent to laminar, but the CFD modeling was carried out for turbulent regime, which may influence the deposition of aerosols due to a higher lateral dispersion. In the future work, the authors will focus on the study of turbulence characteristics and the influence of turbulence model and changes in the turbulent characteristics on the aerosol transport and deposition.

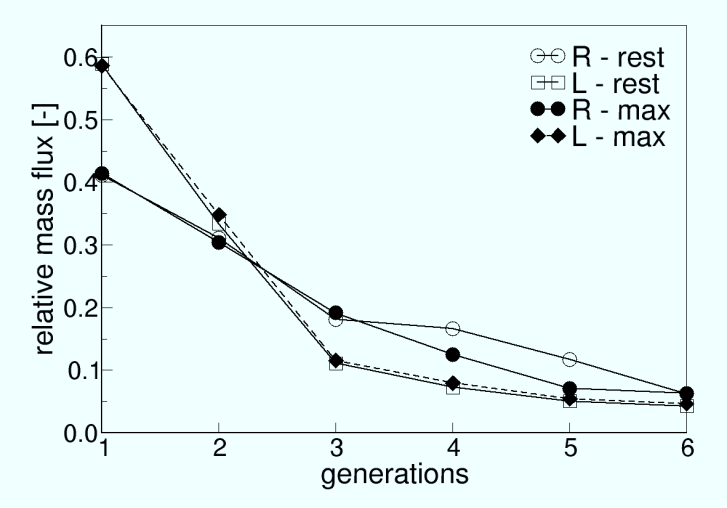

Fig. 3. Relative mass flux in a left and right part of the bronchial tree.

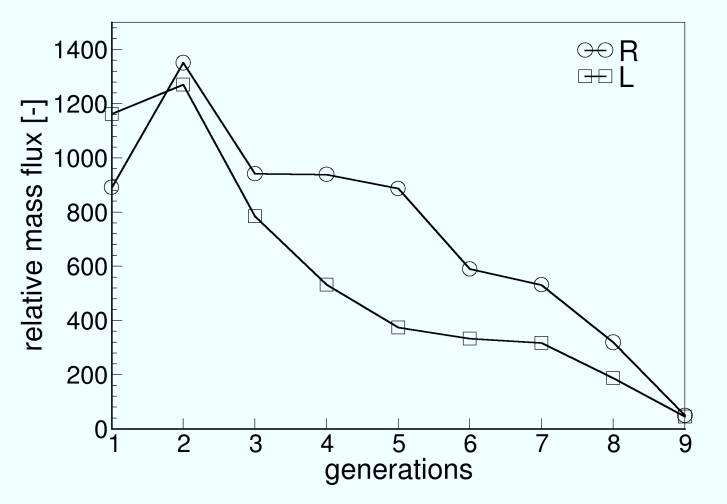

Fig. 4. Reynolds number in different generations at max. inhale velocity – resting condition.

3.1. Aerosol Deposition

Here the deposition of the solid aerosol in three size groups in a transient regime is analysed for the resting condition. The size groups are named D 1, D 5 and D 10 in the graphs corresponding to the PM1, PM5 and PM10 respectively. First the asymmetry in the deposition is shown in fig. 6 for the smallest particles PM1. The relative deposition is shown for the generations 1 to 6, where the deposition count is relative to the overall deposition in the given generation during one breathing cycle. In the first generation the deposition in the right airways

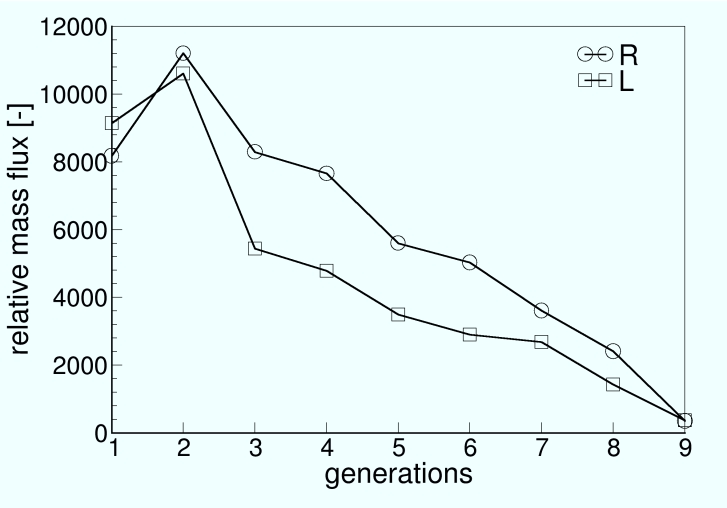

Fig. 5. Reynolds number in different generations at max. inhale velocity – maximum exercise.

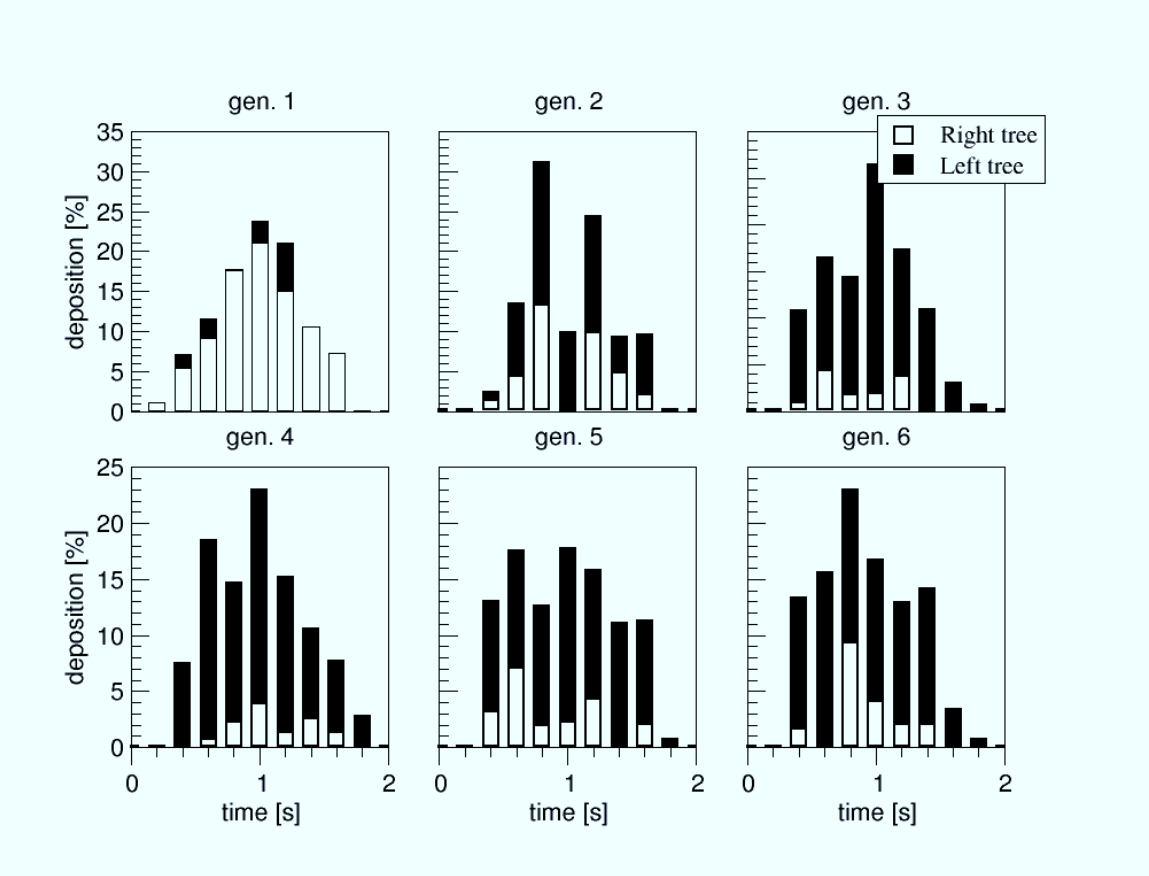

Fig. 6. Relative deposition in left and right generations.

is much larger than the deposition in left airways. We can suspect that the flow pattern behind the bend upstream the plane T3 is responsible for the differences in the deposition. The left sided airways dont show so much directional changes as the right sided airways do, that means the deposition by impaction doesnt appear so frequently and mainly the sedimentation is responsible for the deposition. However in the subsequent generations the deposition is higher in

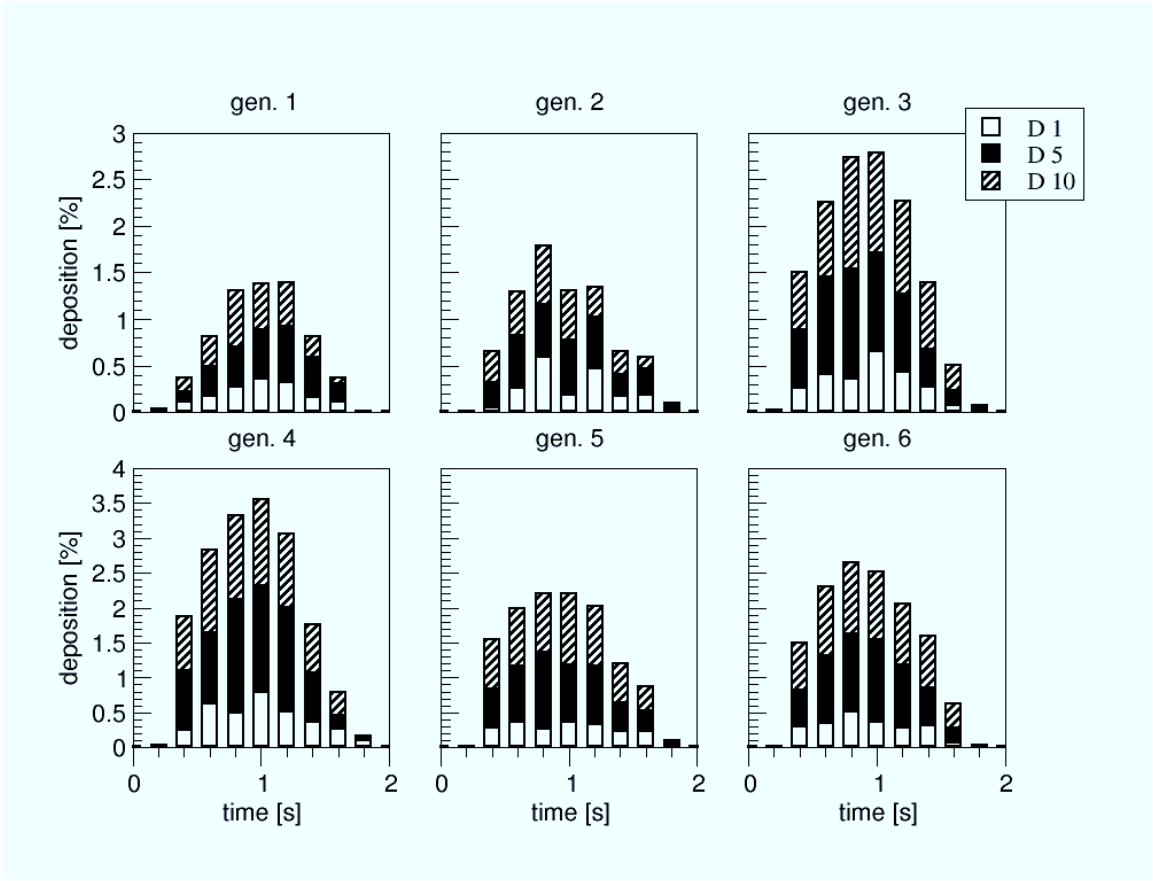

Fig. 7. Relative deposition by mass in subsequent generations.

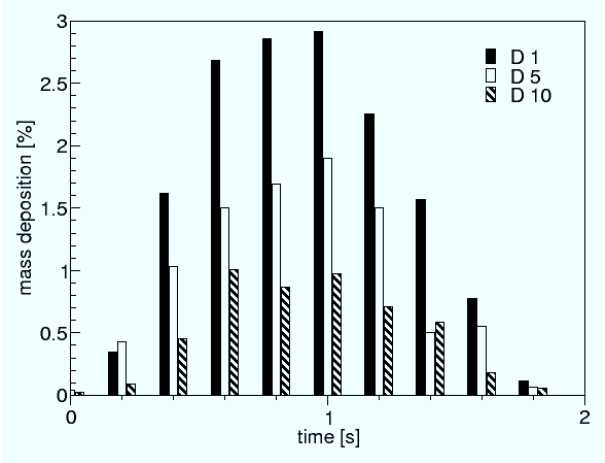

Fig. 8. Relative deposition by mass in subsequent generations.

the left airway during the whole period. Graphs also shows that the deposition roughly follows the sinusoidal profile of the inlet velocity. Again the flow–field differences as well as the different length of the generations are caused by the asymmetry.

To compare different deposition in the generations fig. 7, where the relative mass deposition is plotted with respect to the overall deposition in the whole model during the breathing cycle. While fig. 6 is based on the count of particles, this graphs shows deposited mass of aerosol.

The deposition in the first generation is only 1.5 per cent at the maximum, deposition at further generation is higher. In the forth generation reaches the maximum value of 3.6 per cent and then in the fifth and sixth generation s again lower but always following the sinusoidal profile of the velocity. The highest deposition rate is shown for PM1 in the 3^{rd} and 4^{th} generation which could be attributed to the length of these generations which offer the sufficiently long residence time for the particles to settle down and to several local vortexes that trap the small particles and end their life. Large part of aerosols leaves the airways at the terminating outlets without being deposited. This figure also shows the relative proportions of the size classes on the deposition. Most of the deposited mass consist of the PM5 particles, while the PM1 is deposited the least and at the lowest velocities at the start and end of the inhale phase it is not deposited at all. It concludes that the PM1 particles follows the flow–field to the subsequent generations not included in the model. This result is in accord with the literature and theory showing that the impact of particles on the wall is the main mechanism of deposition in the part of the airways modelled.

Fig. 8 shows the mass based deposition for the part of the trachea modelled. Here mainly PM1 particles are deposited, reaching 50 per cent of the deposition in the trachea. We suspect that the main mechanism is sedimentation at the low velocities greatly enhanced by the turbulent dispersion while heavier particles are carried further downstream. However this effect needs to be studied further employing large–eddy simulation methods. The impact deposition plays also its role, as all three classes follows smoothly velocity profile in time as a result of a particular shape of the airway.

4. Conclusion

Computational modeling of the transport and deposition of aerosols of three size classes PM1, PM5 and PM10 was performed in the model of a respiratory tract acquired from the CT scan of a real human. The model contains 6 generations and isnt idealized as for the individual bifurcations. In this way the surface of the individual airways is not smooth, the individual generations have different cross sections that are not rounded but differ in shape from each other. All these singularities result in more realistic results of the deposition.

We can conclude the following:

- Aerosol deposition is influenced by local obstacles like bends, which results in different deposition rate. Local obstruction can create local vortexes in which smallest particles are trapped and end their life. Thus the deposition can be increased.
- The deposition is also influenced by the asymmetry in the first bifurcation caused by an obstacle in the form of a bend, which results in different flow rates into the left and right airways and thus influences the whole process in the lower airways.
- At the higher flow rate (maximum exercise) the major deposition mechanism is impaction for larger aerosols accompanied by the high deposition of smallest aerosols captured in the local vortexes.
- In general, deposition is higher at the higher flow rate than at the lower flow rate. The major contribution to the deposition at the higher flow rate is impaction that is accompanied by the sedimentation.

Acknowledgements

Financial support from the Czech Ministry of Education and Youth through the COST project 1P05OC028 is gratefully acknowledged.

References

[1] I. Balashazy, T. Heistracher, W. Hofman, Airflow and particle deposition patterns in bronchial airway bifurcation: the effect of different CFD models and bifurcation geometry, J. Aerosol Med. (9) (1996) 287-301.

[2] J.K. Comer, C. Kleinstreuer, C.S. Kim, Aerosol transport and deposition in sequentially bifurcating airways, J. Biomechanical Eng., (122) (2000) 152-158.

[3] D.A. Edwards, Numerical simulation of air and particle transport in the conducting airways, J. Aerosol Med. (9) (1996) 303-316.

[4] A.D. Gosman, E. Ioannides, Aspects of computer simulation of liquid fueled combustors, Paper AIAA-81-0323, 19th Aerospace Science Meeting, St. Louis, MO ,1981.

[5] E.A. Matida, W.H. Finlay, C.F. Lange, B. Grgic, Improved numerical simulation of aerosol deposition in a idealized mouth-throat, J. Aerosol Sci. (35) (2002) 1-19.

[6] R. Sarangapani, A. Wexler, Modelling aerosol bolus dispersion in human airways, J. Aerosol Sci. (30) (1999) 1345-1362.

[7] D.C. Wilcox,TurbulenceModelingforCFD.DCWIndustriesInc.,2ndedition,2000.

[8] Z. Zhang, C. Kleinstreuer,C.S. Kim, A.J. Hickey, Aerosol transport and deposition in a triple bifurcation bronchial airway model with local tumor, Inhalation Toxicology, (14) (2002) 1111-1133.

[9] L. Zheng, C. Kleinstreuer, Z. Zhang, Particle deposition in the human tracheobronchial airways due to transient inspiratory flow patterns, J. Aerosol Science, (38) (2007) 625-644.